

## Polarization retention loss in PbTiO<sub>3</sub> ferroelectric films due to leakage currents

A. Morelli, Sriram Venkatesan, G. Palasantzas,<sup>a)</sup> B. J. Kooi, and J. Th. M. De Hosson  
*Department of Applied Physics, Zernike Institute for Advanced Materials, University of Groningen, Nijenborgh 4, 9747 AG Groningen, The Netherlands and the Netherlands Institute for Metals Research, University of Groningen, Nijenborgh 4, 9747 AG Groningen, The Netherlands*

(Received 7 May 2007; accepted 17 August 2007; published online 16 October 2007)

The relationship between retention loss in single crystal PbTiO<sub>3</sub> ferroelectric thin films and leakage currents is demonstrated by piezoresponse and conductive atomic force microscopy measurements. It was found that the polarization reversal in the absence of an electric field followed a stretched exponential behavior  $1 - \exp[-(t/k)^d]$  with exponent  $d > 1$ , which is distinct from a dispersive random walk process with  $d < 1$ . The latter has been observed in polycrystalline films for which retention loss was associated with grain boundaries. The leakage current indicates power law scaling at short length scales, which strongly depends on the applied electric field. Additional information of the microstructure, which contributes to an explanation of the presence of leakage currents, is presented with high resolution transmission electron microscopy analysis. © 2007 American Institute of Physics. [DOI: 10.1063/1.2794859]

### I. INTRODUCTION

Ferroelectric thin films have attracted significant attention as an active medium for nonvolatile memory devices.<sup>1,2</sup> This is because ferroelectric materials allow control of the spontaneous polarization direction, which corresponds effectively to a data bit, by application of an external electric field, and the corresponding domain wall thickness is typically less than 1 nm.<sup>3</sup> Scanning probe techniques offer an enhanced possibility to create ultrahigh density data storage ( $> 1$  Tbit/in.<sup>2</sup>).<sup>4,5</sup> However, the requirements for nonvolatile data storage are rather stringent including small bit size, fast operating times, reliability related to fatigue, and long-term data retention. Since the remnant polarization directly correlates with the amount of charge that can be detected during the read operation of the memory cell, high values are desired for memory applications. Although the domain switching behavior and stability in relation to writing time and voltage<sup>6,7</sup> are of critical importance, the retention loss is also a crucial factor that needs thorough investigation. The latter is defined as the temporal decrease of the reversed domain size (by lateral movement of the  $c^+/c^-$  domain walls) in the absence of an external field.

Recent retention loss studies of  $\sim 200$  nm thick PbTiO<sub>3</sub> (PTO) thin films fabricated by hydrothermal epitaxy on Nb doped single crystal SrTiO<sub>3</sub> (Ref. 8) showed that nanodomains (36 nm in diameter) did not undergo significant retention loss until  $\sim 1472.2$  h. However, the  $c^+/c^-$  domain walls of the square domains moved laterally after 2 h for  $25 \mu\text{m}^2$  and after 22.22 h for  $1 \mu\text{m}^2$  areas. The retention loss in the square domains proceeded by the lateral movement of the  $c^+/c^-$  domain wall without nucleation of the opposite polarization in the inner domain part.<sup>8</sup> The retention loss was explained by the instability of the curved  $c^+/c^-$  domain wall

and the compressive strain energy with leakage currents being absent. Other studies in polycrystalline films or 90° twinned domain structured PbZr<sub>1-x</sub>Ti<sub>x</sub>O<sub>3</sub> (PZT) films showed that the retention loss nucleated at grain boundaries or twin domain boundaries and progressed via lateral expansion of the reversed portion.<sup>9-12</sup>

It is well known that, from application point of view, films having their  $c$  axis oriented normal to the substrate surface are preferable since their spontaneous polarization lies along this axis. However, in general, some fraction of a film becomes  $a$ -axis oriented during cooling from the growth temperature, particularly at the Curie temperature  $T_C$  to relieve the strain generated during the para- to ferroelectric transition.<sup>13</sup> The volume fraction of  $a$  domain depends mainly on the substrate-film lattice mismatch, thickness of the film, and relaxation of strain by other means such as misfit dislocations. Inhomogeneities in  $a/c$  domain walls can explain the presence of depolarization fields in the film, so that high resolution transmission electron microscopy (HR-TEM) analysis can provide further insight on the relation of retention loss features to microstructure imperfections.

Although for single crystal PTO films the retention loss was attributed to domain wall instability and compressive strain energy without leakage currents,<sup>8</sup> the latter, if present, can also be a serious reason of retention loss and requires further investigations in combination with conductive atomic force microscopy (C-AFM). Leakage currents are supposed to be caused by ion drift and carrier conduction induced by the depolarization field, and degrade the retention characteristics by suppressing the applied fields to the ferroelectric layers. So far detailed studies of leakage effects and retention loss by combination of piezoresponse force microscopy (PFM) and C-AFM are still missing, and it will be the topic of the present paper for the case of an ultrathin PTO film.

<sup>a)</sup> Author to whom correspondence should be addressed. Electronic mail: g.palasantzas@rug.nl

## II. EXPERIMENTAL PART

The single crystal PTO film of 30 nm in thickness was fabricated by pulsed laser deposition onto  $\text{DyScO}_3$  with a 5 nm  $\text{SrRuO}_3$  film as an electrode for PFM measurements. Out of a batch of five samples (and with different PTO thicknesses in the range of  $\sim 5$ –30 nm) only the present showed retention loss which was thoroughly investigated. The Dimension 3100 SPM was used for the PFM and C-AFM measurements. The PFM measurements of the out-of-plane polarization were performed with conductive Si cantilevers of spring constant of 40 N/m, which are sufficiently stiff to reduce the influence of nonlocal electrostatic effects causing cantilever buckling oscillations.<sup>14</sup> The ac peak-to-peak voltage was 4 V applied on the tip, and with frequency of 5 kHz. Local polarization reversal of the as deposited PTO films was performed by applying a dc voltage of  $-3.5$  V on the tip. The C-AFM measurement was performed using conductive Si tips coated with doped diamondlike carbon films and cantilevers with spring constant about 40 N/m. The sample bias voltage during C-AFM measurements was varied from 1.8 to 2.05 V.

The TEM cross section specimens were prepared by the conventional method involving cutting, grinding, polishing, dimpling, and ion milling. A precision ion polishing system (Gatan model 691) with 4 kV  $\text{Ar}^+$  beams having incident angle of  $8^\circ$  on both sides was used. The observations are performed with a JEOL 2010F electron microscope at an accelerating voltage of 200 kV. The as deposited film had only a  $c^-$  monodomain at the virgin state, while HRTEM showed also the presence of  $a$  domains in contrast to PTO films in Ref. 8 which were  $c$ -domain type only.

## III. PIEZORESPONSE AND CONDUCTIVE ATOMIC FORCE MICROSCOPY ANALYSIS

Figure 1 shows the polarization reversal to its original state within a short period of time ( $<1$  h). This reversal occurs in the absence of an external electric field and is driven primarily by internal depolarizing fields, elastic strain fields, and leakage currents. Plotting the area of the reversed state versus time, we obtain an exponential growth. From this macroscopic measurement, one obtains an average of the retention characteristics of relatively large area. Although in some cases the retention loss fits a log-time dependence, in most cases appears to fit a stretched exponential  $\propto 1 - \exp[-(t/k)^d]$ ,<sup>9</sup> which is also the case in the present study.

Exponents  $d < 1$  have been attributed to characterize as a dispersive transport or random walk-type process as for the case for polycrystalline PZT films ( $d=0.24$ – $0.68$ ).<sup>9</sup> In our case we have obtained  $d=1.23$  excluding that the retention loss occurs by a random walk process. This is expected since in our case leakage currents were detected, and they can be ascribed as the significant cause of back switching by redistributing the charges and suppressing the electric fields built in the ferroelectric layer.<sup>15</sup> Notably the effective inversion time  $k$  from the fit in Fig. 1 is  $k=2395$  s (0.66 h). This is a much shorter period than the retention time without leakage effects in PTO (more than 2 h depending on domain size),<sup>8</sup> and the retention time in polycrystalline PZT films.<sup>9</sup> Note,

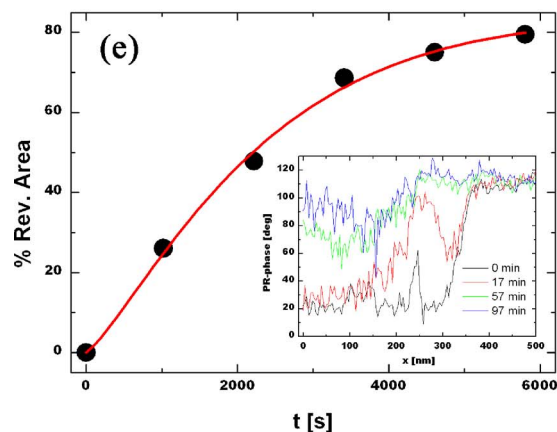
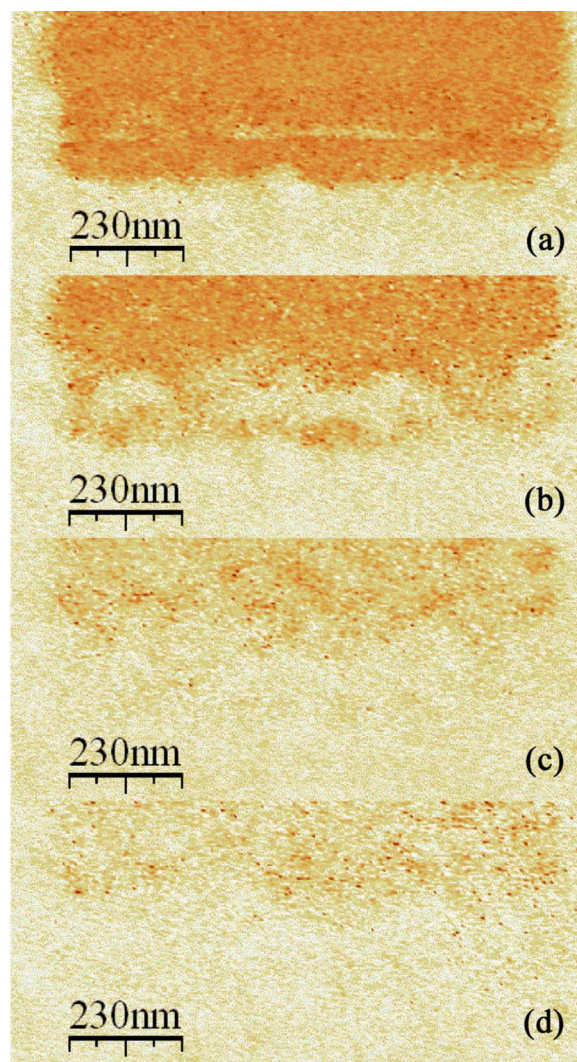


FIG. 1. (Color online) Piezoresponse (PR) phase images acquired after polarization reversal: (a) after poling, (b) 17, (c) 57, and (d) 97 min later. (e) Plot of area percentage as a function of time evaluated by PR phase images taken after polarization reversal by poling the tip at  $-3$  V over a  $1 \mu\text{m}^2$  area. (a)–(d) show snapshots of this area. The fit parameters are shown also in this schematic with the fit function  $A(1 - \exp[-(t/k)^d])$  and fit parameters  $d = 1.23 \pm 0.14$ ,  $A = 84.2 \pm 4.6$ , and  $k = 2395.8 \pm 245.2$  s. The inset shows line profiles of the PR phase with an initial maximum phase difference approximately  $100^\circ$ .

however, that the PTO samples in Ref. 8 were  $c$ -domain type only, while in our case the presence of  $a$  domains (as will be discussed in more detail in a following paragraph by HR-



TEM), which makes any comparison possible only in a qualitative sense only. Therefore, leakage currents can affect polarization dynamics more significantly than other instability and/or grain boundaries related mechanisms.

Moreover, as Fig. 2 indicates, the topography changes (expands) with the domain reversal and formation of the  $c^+$  domain. The expansion is approximately 1.5–2 nm, indicating that the  $c^+$  domain is under stress, which further could augment the retention loss<sup>8</sup> in combination with any nonuniform charge on the  $c^+/c^-$  domain. Indeed, when an external electric field is applied via the AFM tip, the electric field distribution in a film is inhomogeneous, and as a result the reversed domains have a curved  $c^+/c^-$  domain wall, and extend to the bottom electrode.<sup>8</sup> The head-to-head polarization structure leads to positive charges along the curved domain wall. The electrostatic energy caused by the depolarization fields makes the curved  $c^-/c^+$  domain wall energy higher than the straight domain wall energy that contributes to the driving force for the domain back reversal and retention loss. This is the case if these depolarization fields are not compensated by free charges that exist intrinsically in the PTO film (corresponding to films with significant remnant polarization and no leakage currents). On the other hand, in our case leakage currents could compensate charges along the  $c^+/c^-$  boundary, minimizing the domain wall instability due to the depolarization field.

Three dimensional maps of the leakage currents are shown in Fig. 3, where it is found a strong dependence on the applied potential close to 2 V. The electric field  $E$  in ferroelectric thin films induced by the bias voltage between AFM tip and bottom electrode can be large enough to bring surface charges and charge injections on ferroelectric thin films.<sup>16</sup> For SBT ( $\text{SrBi}_2\text{Ta}_2\text{O}_6$ ) films (40 nm thick) the leakage current was calculated by the consideration of Schottky emission for a bias  $>2.0$  V, and it was found large enough to induce surface charges.<sup>16</sup> For the PTO film the leakage current grows very fast as we approached 2 V [Fig. 3(c)]. The average current density for each scanned area was calculated by considering the local contact area  $\approx \pi R^2$  (radius of tip curvature  $R=200$  nm) as  $J=\langle I \rangle / \pi R^2$ . The current density  $J$  vs  $E$  plot [Fig. 3(d)] shows a steep increase at 2.05 V, confirming Schottky emission to occur for a bias  $>2.0$  V.

In addition, an analysis of current-difference (CD) correlation function  $H(r)=\langle [I(r)-I(0)]^2 \rangle$  (with  $\langle \dots \rangle$  indicating ensemble average over the 512 lines along the fast scan direction) was performed in order to obtain information about the leakage current fluctuations [see Fig. 3(e)].<sup>17,18</sup> The CD correlation functions were shown to follow the scaling behavior  $H(r)=r^{2a}$  if  $r \ll \xi$  and  $H(r)=2w_l^2$  if  $r \gg \xi$ .  $w_l = \langle [I - \langle I \rangle]^2 \rangle^{1/2}$  is the saturated current fluctuation, which is extracted by the plateau value of the CD log-log plot. The exponent  $a$  is determined by the slope ( $=2a$ ) of the linear part of  $H(r)$ , and the correlation length  $\xi$  is determined at the crossover between linear fit and the saturation regime that gives  $w_l$ . Notably the correlation length has almost constant value  $\xi \approx 25$  nm, while  $w_l$  and  $a$  grow with increasing electric field  $E$  [Fig. 3(f)].

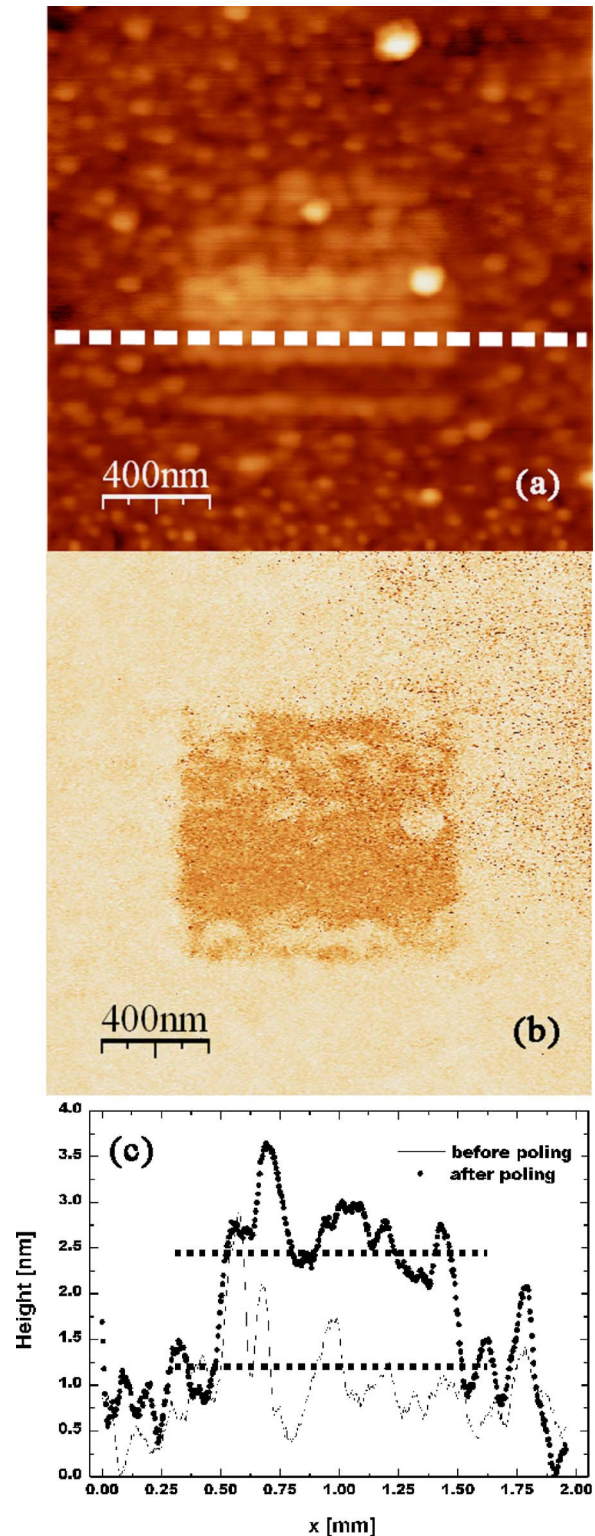


FIG. 2. (Color online) (a) Topography with area polarization reversal is shown. The section taken horizontally in the center is where the vertical displacement of about 1.5–2 nm is estimated; (b) phase map; (c) line profiles along the indicated line in (a). The dotted lines are a guide to show qualitatively the change in topography upon intentional polarization reversal.

#### IV. TRANSMISSION ELECTRON MICROSCOPY ANALYSIS

The TEM bright field image of the same PTO film (analyzed by PFM and C-AFM in Sec. III) is shown in Fig. 4(a).

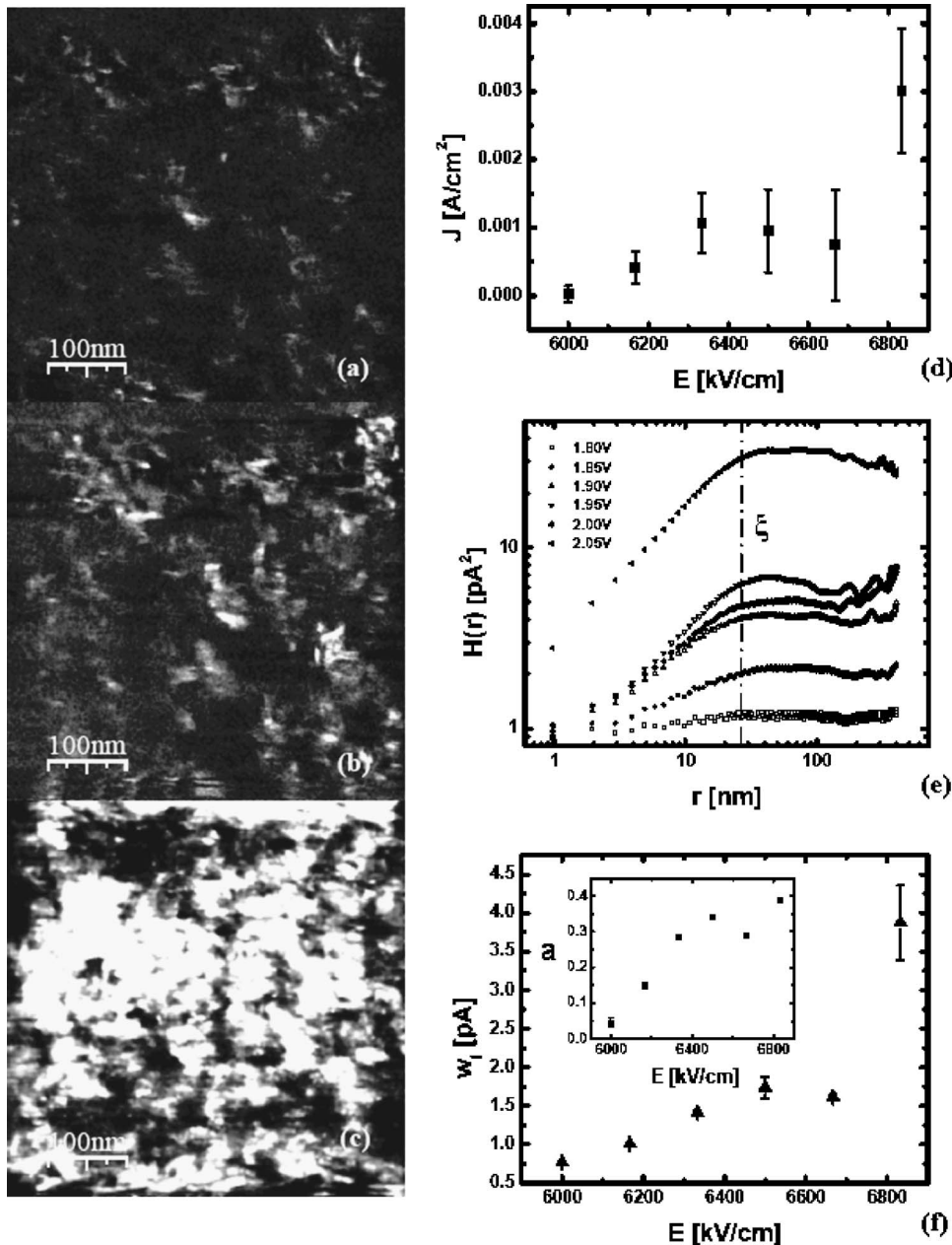


FIG. 3. C-AFM measurement over an area of  $500 \times 500 \text{ nm}^2$ , scale of all current images is  $0\text{--}3.5 \text{ pA}$  at (a)  $1.8 \text{ V}$ , (b)  $1.85 \text{ V}$ , and (c)  $2.05 \text{ V}$ , showing strong leakage currents. (d) The plot shows the density of current (for a tip radius of  $200 \text{ nm}$ ) vs the applied electric field. (e) Current-current correlation functions plots. The vertical line shows the correlation length  $\xi$ . (f) Current fluctuation  $w_l$  and exponent  $a$  (inset) as calculated from the CD correlation functions.

The  $\text{DyScO}_3$  has an orthorhombic structure with the following lattice constants (at room temperature):  $a=5.440 \text{ \AA}$ ,  $b=5.713 \text{ \AA}$ ,  $c=7.887 \text{ \AA}$ .<sup>19</sup> (110)-oriented  $\text{DyScO}_3$  has nearly a square in-plane lattice with  $a_{\parallel}=3.944 \text{ \AA}$ . The  $\text{PbTiO}_3$  has a tetragonal structure with (at room temperature)  $a=b=3.894 \text{ \AA}$ ,  $c=4.140 \text{ \AA}$ .<sup>20</sup> From the lattice parameters we can expect a lattice mismatch of about 1.4% between the substrate and the  $a$  axis of PTO. The corresponding strain results in the formation of  $a$  domains in the film. These domains can be clearly identified in the TEM images; for example, in the bright field and high resolution images in Figs. 4(a) and 4(b), respectively. TEM images indicate that the  $a$  domains have a typical width of  $7\text{--}8 \text{ nm}$ , but also domains with a width of only  $2 \text{ nm}$  have been observed. The distance between neighboring  $a$  domains is typically  $30 \text{ nm}$  and although they may look periodically spaced, some clear variations in distances (typically  $\pm 10 \text{ nm}$ ) were observed.

The lateral resolution by PFM in out-of-plane (as in

Figs. 1 and 2) or lateral mode is presently more than  $30 \text{ nm}$  (mainly due to finite tip size effects). As a result it cannot provide information of the  $a$  domains since their width ( $< 9 \text{ nm}$ ) is far less than the AFM tip dimensions and thus the PFM resolution. Therefore, only contrast due to out of plane polarization of the  $c$  domains is possible (e.g., Figs. 1 and 2). Nevertheless, HRTEM shows convincingly the presence of  $a$ - $c$  domain configurations. The  $c/a$  ratio of the film derived from HRTEM images is  $1.07 (\pm 0.01)$ , which is in agreement with the theoretical value of  $1.063$ . The predicted tilt of the unit cell within the  $a$  domain with respect to the  $c$  matrix of the PTO film was calculated from the relation  $2 \tan^{-1}(c/a) - 90^\circ$ . The latter yielded  $3.8^\circ$ , which is close to the theoretical value of  $3.5^\circ$ . Furthermore, a clear contrast of dislocations within the PTO film has also been observed.

Careful analysis of  $a$  domains using HRTEM indicates that their width is in many instances not constant, but de-



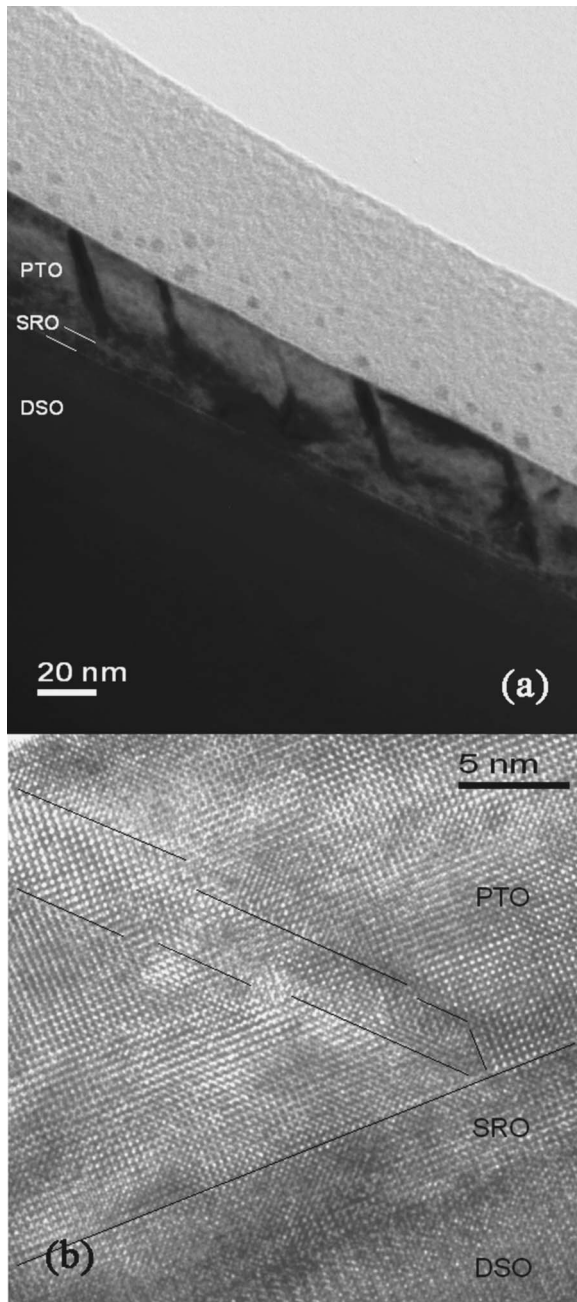


FIG. 4. TEM images of a 30 nm  $\text{PbTiO}_3$  film on 5 nm  $\text{SrRuO}_3$  on a  $\text{DyScO}_3$  substrate. (a) Bright field image showing the presence of a large fraction of  $a$  domains. (b) High resolution image showing steps in the domain wall.

creases from top to bottom, e.g., the domains have a (slight) wedge shape. The major part of the domain walls are formed by  $\{101\}$  planes along which the  $a$  and  $c$  domains can perfectly match. However, the varying width of the domains also causes steps in the domain wall. In Fig. 4(b) such steps are present in the regions, where the indicated lines giving the position of the domain wall are not continuous. Steps are not always precisely located in the TEM images, since can change their position across the thickness of the HRTEM image, i.e., the two-dimensional projection of the three-dimensional object causes blurring of the HRTEM image in the step region. The steps cause local distortion of the crystal structure and may also lead to local changes in stoichiometry of the PTO. The observed retention loss due to leakage cur-

rents may be attributed to the presence of (a significant density of) these steps. This explanation is supported by the fact that cross-sectional TEM images of another 30 nm PTO film on  $\text{DyScO}_3$  (having in this case a thicker  $\sim 30$  nm thick  $\text{SrRuO}_3$  bottom electrode) showed clearly more parallel walls (i.e., less or absence of steps) between the  $a$  and  $c$  domains. In addition, these samples did not show any retention loss by the same PFM/C-AFM analysis as performed in the present study and therefore the presence of leakage currents.

## V. CONCLUSIONS

From the studies discussed here, it appears that fast spontaneous polarization reversal can be also dominated by leakage currents. It was found that the polarization reversal in the absence of an electric field followed a stretched exponential behavior with an exponent  $d > 1$ , which can be distinct from a dispersive random walk process with  $d < 1$  to characterize retention loss due to grain boundaries as in polycrystalline PZT films. Moreover, the retention loss was found to be much faster than that of nonleaking PTO thin films.<sup>8</sup> The leakage current indicated power law scaling at short length scales, which strongly depends on the applied electric field. Further studies are in progress to understand theoretically any possible relation of the leakage current parameters ( $w_l$ ,  $a$ , and  $\xi$ ) related to the internal film structure and the corresponding temporal evolution of the back switched area (due to leakage) as it is shown, for example, in Fig. 1. In any case, the presence of leakage currents possibly arises by the presence of defects in the domain walls between  $a$  and  $c$  domains, which are confirmed with TEM analysis.

## ACKNOWLEDGMENT

We would like to acknowledge support by the Zernike Institute for Advanced Materials through the MSC+ program.

- <sup>1</sup>J. F. Scott and C. A. Araujo, *Science* **246**, 1400 (1989).
- <sup>2</sup>C. A. Paz de Araujo, J. D. Cuchiaro, L. D. McMillan, M. C. Scott, and J. F. Scott, *Nature (London)* **374**, 627 (1995).
- <sup>3</sup>F. Jona and G. Shirane, *Ferroelectric Crystals* (Pergamon, Oxford, 1962), p. 46.
- <sup>4</sup>T. Hidaka, T. Mayurama, M. Saitoh, N. Mikoshiba, M. Shimizu, T. Shiosaki, L. A. Wills, R. Hiskes, S. A. Dicarolis, and J. Amano, *Appl. Phys. Lett.* **68**, 2358 (1996).
- <sup>5</sup>C. H. Ahn, T. Tybell, L. Antognazza, K. Char, R. H. Hammond, M. R. Beasley, Ø. Fisher, and J.-M. Triscone, *Science* **276**, 1100 (1997).
- <sup>6</sup>P. Paruch, T. Tybell, and J.-M. Triscone, *Appl. Phys. Lett.* **79**, 530 (2001).
- <sup>7</sup>Y. Cho, K. Fujimoto, Y. Hiranaga, Y. Wagatsuma, A. Onoe, K. Terabe, and K. Kitamura, *Nanotechnology* **14**, 637 (2003).
- <sup>8</sup>W. S. Ahn, W. W. Jung, S. K. Choi, and Y. Cho, *Appl. Phys. Lett.* **88**, 082902 (2006).
- <sup>9</sup>A. Gruverman, H. Tokumoto, A. S. Prakash, S. Aggarwal, B. Yang, M. Wuttig, R. Ramesh, O. Auciello, and T. Venkatesan, *Appl. Phys. Lett.* **71**, 3492 (1997).
- <sup>10</sup>D. Fu, K. Suzuki, K. Kato, M. Minakata, and H. Suzuki, *Jpn. J. Appl. Phys., Part 1* **41**, 6724 (2002).
- <sup>11</sup>C. S. Ganpule, V. Nagarajan, S. B. Ogale, A. L. Roytburd, E. D. Williams, and R. Ramesh, *Appl. Phys. Lett.* **77**, 3275 (2000).
- <sup>12</sup>C. S. Ganpule, A. L. Roytburd, V. Nagarajan, B. K. Hill, S. B. Ogale, E. D. Williams, R. Ramesh, and J. F. Scott, *Phys. Rev. B* **65**, 014101 (2001).
- <sup>13</sup>S. Stemmer, S. K. Streiffer, F. Ernst, M. Rühle, W.-Y. Hsu, and R. Raj, *Solid State Ionics* **75**, 43 (1995).
- <sup>14</sup>S. V. Kalinin and D. A. Bonnell, in *Electric Scanning Probe Imaging and*

*Modification of Ferroelectric Surfaces*, in *Nanoscale Characterization of Ferroelectric Materials*, edited by M. Alexe and A. Gruverman (Springer, Berlin, 2004), pp. 1–39.

- <sup>15</sup>M. Molotskii, A. Agronin, P. Urenski, M. Shvebelman, G. Rosenman, and Y. Rosenwaks, *Phys. Rev. Lett.* **90**, 107601 (2003).
- <sup>16</sup>J. Y. Son, K. Kyhm, and J. H. Cho, *Appl. Phys. Lett.* **89**, 092907 (2006).
- <sup>17</sup>P. Meakin, *Phys. Rep.* **235**, 1991 (1994); J. Krim and G. Palasantzas, *Int. J. Mod. Phys. B* **9**, 599 (1995).
- <sup>18</sup>Y. P. Zhao, G. C. Wang, and T. M. Lu, in *Characterization of Amorphous and Crystalline Rough Surface: Principles and Applications*, edited by R. Celotta and T. Lucatorto (Academic, San Diego, 2001).
- <sup>19</sup>J. H. Haeni, P. Irvin, W. Chang, R. Uecker, P. Reiche, Y. L. Li, S. Choudhury, W. Tian, M. E. Hawley, B. Craigo, A. K. Tagantsev, X. Q. Pan, S. K. Streiffer, L. Q. Chen, S. W. Kirchoefer, J. Levy, and D. G. Schlom, *Nature (London)* **430**, 758 (2004).
- <sup>20</sup>G. Shirane, S. Hoshino, and K. Suzuki, *Phys. Rev.* **80**, 1105 (1950).